Synthesis and Properties of New Side-Chain Liquid Crystalline Polymers by Metathesis Cyclopolymerization

Sang-Jun Choi,† Sung-Hyun Kim,† Wonsool Ahn,‡ Hyun-Nam Cho,‡ and Sam-Kwon Choi*,†

Department of Chemistry, Korea Advanced Institute of Science and Technology, 373-1 Kusung-Dong, Yusung-Gu, Taejon, Korea, and Polymer Materials Laboratory, Korea Institute of Science and Technology, P.O. Box 131, Cheangyangri, Seoul, Korea

Received November 15, 1993; Revised Manuscript Received May 3, 1994®

ABSTRACT: New thermotropic side-chain liquid crystalline polymers containing a poly(dipropargylamine) backbone were prepared by metathesis polymerization with transition metal catalysts. It was found that the $MoCl_5$–$EtAlCl_2$ catalyst system was very effective for the cyclopolymerization of the presently investigated monomers. The resulting polymers exhibited good solubility in common organic solvents such as tetrahydrofuran (THF), chloroform, etc. and could be cast on glass plates to give dark-brown films. The structure of the polymers was confirmed by IR, UV–visible, and ^1H and ^{13}C NMR spectra. The number-average molecular weight ($\bar{M}_n$) values of the polymers were in the range 6.49×10^3–1.8×10^4 relative to polystyrene standards by GPC. The thermal properties of the monomers and the polymers synthesized were analyzed by differential scanning calorimetry (DSC), cross-polarized optical microscopy, and X-ray diffraction analysis. Both monomers and polymers displayed enantiotropic liquid crystallinity. The room-temperature conductivities of the undoped and I_2-doped polymers were found to be about 10^{-11} and 10^{-3} S/cm, respectively.

Introduction

Thermotropic side-chain liquid crystalline polymers are receiving considerable research interest for special applications, e.g., in data storage systems, in piezo-, pyro-, and ferroelectric devices, and in systems requiring nonlinear optical characteristics.[1] Recently, a large variety of side-chain liquid crystalline (LC) polymers have been extensively investigated because of their theoretical and technological significance.[1-4] To obtain the mesophases of these polymers, introduction of flexible spacer groups between the polymer main chain and the mesogenic side chain is necessary to decouple the motions of the backbone component from those of the anisotropically oriented mesogenic group.[5]

Most of the studies of side-chain LC polymers to date have been concerned with materials in which the mesogenic groups are attached to a flexible polymer backbone (polyacrylates, polymethacrylates,[3,4] polysiloxanes,[6,7] etc.). There are numerous recent examples of side-chain LC polymers prepared by radical, cationic, group-transfer, and ring-opening metathesis polymerization.[8-10] However, to our knowledge there are very few reports in the literature concerning the use of a rigid polymer backbone for side-chain LC polymers.[11-14] Furthermore, systematic studies to prepare side-chain LC polymers with electrically conducting properties by metathesis polymerization are relatively rare.[14,15]

In our previous work, we reported the synthesis and characterization of poly(dipropargylamide) containing the 4-cyano-4′-hydroxybiphenyl mesogenic group with methylene units as the flexible spacer in order to obtain thermotropic LC mesomorphism from such a rigid polymer backbone.[16]

In this paper, we describe in detail the results on the preparation and properties of another series of a novel class of thermotropic side-chain LC monomers with amine functional groups which are introduced for the first time in metathesis cyclopolymerization and their polymers which have a poly(dipropargylamine) backbone with electrically conducting properties.

Experimental Section

Materials. Tungsten(VI) and molybdenum(V) chlorides (Aldrich Chemical Co., resublimed, 99.9%) were used without further purification. Ethylaluminum dichloride (Aldrich Chemical Co.) was used without further purification, and tetrabutyltin was distilled under reduced pressure. All solvents were used after purification according to conventional methods. 4-Aminophenol, 1,6-dibromohexane, and 1,12-dibromododecane (all from Aldrich Chemical) were used without further purification. 4-Cyano-4′-hydroxybiphenyl was obtained from Tokyo Kasei and was used as received.

Instruments. ^1H and ^{13}C NMR spectra were recorded with a Bruker AM-300 spectrometer, and chemical shifts are reported in ppm units with tetramethylsilane as an internal standard. Infrared spectra were measured as a neat oil or as KBr pellets on a Bomen spectrometer, and frequencies are given in reciprocal centimeters. A Shimadzu UV-3100S spectrometer was used for UV spectral data. The number-average molecular weight ($\bar{M}_n$) and polydispersities were determined in THF solvent with a Waters GPC-150C calibrated with polystyrene standards. A Perkin-Elmer DSC-IV differential scanning calorimeter was used to obtain the DSC thermograms with heating rates of 10 °C/min in a nitrogen atmosphere. A Leitz Ortholux-II optical microscope equipped with a Mettler FP-80 hot stage was used in the cross-polarized mode for visual observation of the thermotropic behavior and optical texture of the monomers and polymers. X-ray diffraction measurements were performed with nickel-filtered Cu Kα radiation with a Rigaku powder diffractometer at room temperature. The electrical conductivity was determined with an Ando AG-4303 LCR meter at a fixed frequency of 100 Hz with an applied voltage of 1 V.

Synthesis of Monomers. 4-(Dipropargylamino)phenol (I). 4-Aminophenol (5 g, 46 mmol) and propargyl bromide (30 g, 0.2 mol) were stirred in CH_3CN (150 mL) at reflux for 20 h. The reaction mixture was washed with water and extracted with methylene chloride. The solvent was removed with a rotatory evaporator, and the crude product was purified by column chromatography on silica gel with ethyl acetate and hexane (1:2) as eluent; yield 40%. ^1H NMR ($CDCl_3$): δ (ppm) 3.1 (t, $\equiv$CH, 2H), 4.5 (d, $CH_2C\equiv$, 4H), 7.2 (d, aromatic protons, 2H), 7.4 (d, aromatic protons, 2H), 8.4 (b, OH, 1H).

4-((6-Bromohexyl)oxy)-4′-cyanobiphenyl (II). This compound was prepared by refluxing a phenolate solution obtained

* To whom all correspondence should be addressed.
† Korea Advanced Institute of Science and Technology.
‡ Korea Institute of Science and Technology.
® Abstract published in *Advance ACS Abstracts*, July 15, 1994.

0024-9297/94/2227-4871$04.50/0

Scheme 1

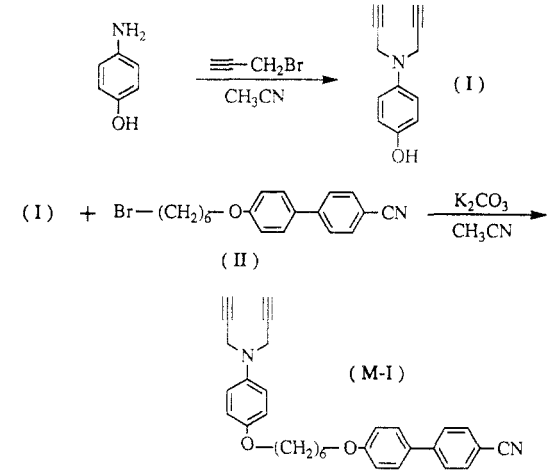

Scheme 2

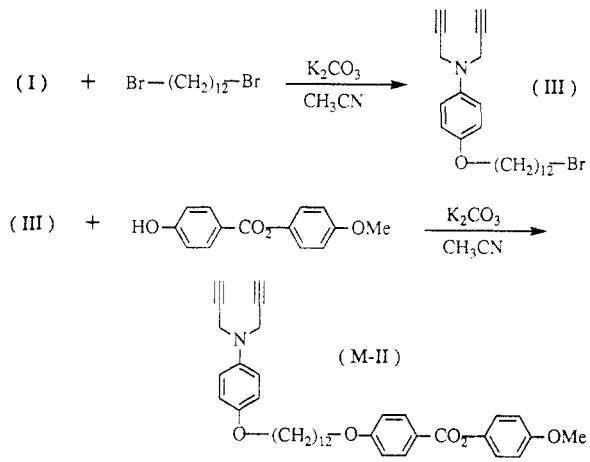

by the interaction of 4-cyano-4′-hydroxybiphenyl and K_2CO_3 with 1,6-dibromohexane in acetone for 20 h. After the reaction was over, chloroform and water were added to the reaction mixture and the whole solution was shaken. The organic layer was separated, washed with water, and dried over anhydrous magnesium sulfate. The solvent was removed with a rotatory evaporator, and the crude product was purified by column chromatography on silica gel with ethyl acetate and hexane (1:3) as eluent; yield 85%. ^{1}H NMR ($CDCl_3$): δ (ppm) 1.5–1.7 (m, $(CH_2)_2$, 4H), 1.8–2.0 (m, $(CH_2)_2$, 4H), 3.4 (t, ≡CH, 2H), 4.0 (d, CH_2≡, 2H), 7.0 (d, aromatic protons, 2H), 7.5 (d, aromatic protons, 2H), 7.6 (t, aromatic protons, 4H).

12-Bromododecanyl 4-(Dipropargylamino)phenyl Ether (III). A mixture of 4-(dipropargylamino)phenol (I, 5 g, 27 mmol), 1.12-dibromododecane (20 g, 61 mmol), and anhydrous K_2CO_3 (10 g) in 150 mL of CH_3CN was refluxed with stirring for 20 h. The mixture was poured into water and extracted with methylene chloride. The extract was dried over anhydrous magnesium sulfate and evaporated to dryness. A crude product was purified by column chromatography on silica gel using a 25:75 mixture of ethyl acetate and hexane as eluent; yield 75%. ^{1}H NMR ($CDCl_3$): δ (ppm) 1.2–1.5 (m, $(CH_2)_8$, 16H), 1.6–1.8 (m, $(CH_2)_2$, 4H), 2.2 (t, ≡CH, 2H), 3.4 (t, CH_2Br, 2H), 3.9 (t, OCH_2, 2H), 4.0 (d, CH_2C≡, 2H), 6.8 (d, aromatic protons, 2H), 6.9 (d, aromatic protons, 2H).

((4′-Cyano-(1,1′-biphenyl)-4-yl)oxy)hexyl 4-(Dipropargylamino)phenyl Ether (M-I). The procedure for the synthesis of M-I is illustrated in Scheme 1. A mixture of 4-(dipropargylamino)phenol (I, 3 g, 16.2 mmol), compound II (5.8 g, 16.2 mmol), and anhydrous K_2CO_3 (5 g) in 150 mL of CH_3CN was refluxed with stirring for 24 h. The reaction was checked by TLC. After cooling, the salt was filtered. The filtrate was purified by column chromatography on silica gel using a 35:65 mixture of ethyl acetate and hexane as eluent, which was further purified by recrystallization from ethanol; yield 83%. ^{1}H NMR ($CDCl_3$): δ (ppm) 1.4–1.7 (m, $(CH_2)_2$, 4H), 1.7–1.9 (m, $(CH_2)_2$, 4H), 2.2 (t, ≡CH, 2H),3.9 (t, OCH_2, 2H), 4.0 (d, CH_2C≡, 4H), 4.0 (t, OCH_2, 2H),

Scheme 3

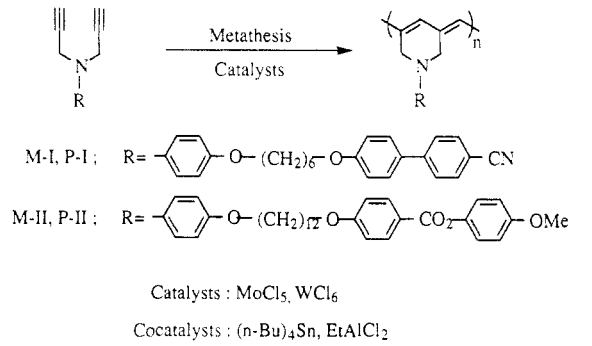

6.8–7.0 (m, aromatic protons, 6H), 7.5–7.7 (m, aromatic protons, 6H). IR (cm^{-1}): 3280 (≡CH); 2225 (CN); 1605, 1525 (C–C aromatics). ^{13}C NMR ($CDCl_3$): 41.5 (CH_2C≡), 72.8 (≡CH), 79.3 (C≡CH).

4-Methoxyphenyl ((((4-(Dipropargylamino)phenyl)oxy)dodecanyl)oxy)benzoate (M-II). The procedure for the synthesis of M-II is illustrated in Scheme 2. A mixture of compound III (4 g, 9.3 mmol), 4-methoxyphenyl 4-hydroxybenzoate[16] (3.4 g, 14 mmol) and anhydrous K_2CO_3 (5 g) in 150 mL of CH_3CN was refluxed with stirring for 24 h. The reaction was checked by TLC. After cooling, the salt was filtered. The filtrate was purified by column chromatography on silica gel using a 35:65 mixture of ethyl acetate and hexane as eluent, which was further purified by recrystallization from ethanol; yield 78%. ^{1}H NMR ($CDCl_3$): δ (ppm) 1.3–1.7 (m, $(CH_2)_8$, 1.7–1.9 (m, $(CH_2)_2$, 4H), 2.2 (t, ≡CH, 2H), 3.8 (s, OCH_3, 3H), 3.9 (t, OCH_2, 2H), 4.0 (d, CH_2C≡, 4H), 4.0 (t, OCH_2, 2H), 6.8–7.0 (m, aromatic protons, 8H), 7.0–7.1 (d, aromatic protons, 2H), 8.0–8.1 (d, aromatic protons, 2H). IR (cm^{-1}): 3280 (≡CH); 1725 (CO_2); 1605, 1525 (C–C aromatics). ^{13}C NMR ($CDCl_3$): 41.5 (CH_2C≡), 72.8 (≡CH), 79.2 (C≡CH), 165.3 (C=O).

Polymerization. Catalyst preparation and polymerization were carried out in a dry nitrogen atmosphere. Transition metal halides and organometallic compounds were dissolved in each solvent to make 0.05 and 0.5 M solutions before use. A typical polymerization procedure is as follows: solvent, catalyst solution, and, when needed, cocatalyst solution were injected into a 20 mL ampule equipped with a rubber septum in the order given. When a cocatalyst was used, the catalyst system was aged at 30 °C for 15 min. Finally, the monomer dissolved in each solvent was injected into the polymerization ampule. After the reaction mixture was allowed to react at 60 °C for 24 h, the polymerization was terminated by adding a small amount of methanol. The resulting polymer was dissolved in chloroform and precipitated with a large excess of methanol. The polymer was filtered from the solution and dried under vacuum at 40 °C for 24 h. Polymer yield was determined by gravimetry.

Results and Discussion

Scheme 3 outlines the cyclopolymerization of the monomers with transition metal catalyst systems.[18]

The polymerization of M-I was carried out with $MoCl_5$- and WCl_6-based catalysts, and their results are summarized in Table 1. The catalytic activity of $MoCl_5$ was greater than that of WCl_6. As shown in Table 1, $EtAlCl_2$ exhibited excellent cocatalyst activity compared with $(n\text{-Bu})_4Sn$ for the polymerization of M-I. When the polymerization was carried out with $MoCl_5$–$EtAlCl_2$, a quantitative polymer yield was obtained.

Table 2 lists the results of the polymerization of M-II by using $MoCl_5$- and WCl_6-based catalysts. These results are similar to those for the polymerization of M-I. The $\bar{M}_n$ of P-II was in the range (1.3–1.8) × 10^4 with polystyrene standards.

The ^{1}H NMR spectra of M-I and P-I are shown in Figure 1. As the polymerization proceeded, the acetylenic proton peak at about 2.2 ppm disappeared and new vinylic proton peaks appeared at 6.3–6.7 ppm together with aromatic proton peaks. Also, the methylene proton peaks adjacent

Table 1. Polymerization of M-I with Various Transition Metal Catalysts[a]

exp. no.	cat. system[b] (mole ratio)	[M]/[C][c]	$[M]_0$[d]	polym yield (%)[e]	$\bar{M}_n \times 10^{-3}$ [f]	$\bar{M}_w/\bar{M}_n$ [f]
1	$MoCl_5$	50	0.25	95	7.7	2.7
2	$MoCl_5$	100	0.25	76	7.2	2.8
3	$MoCl_5$	50	0.5	90	7.8	3.1
4	$MoCl_5$–$(n\text{-Bu})_4Sn$ (1:4)	50	0.25	80	6.7	3.0
5	$MoCl_5$–$EtAlCl_2$ (1:4)	50	0.25	100	6.49	2.4
6	WCl_6	50	0.25	trace		
7	WCl_6–$(n\text{-Bu})_4Sn$ (1:4)	50	0.25	trace		
8	WCl_6–$EtAlCl_2$ (1:4)	50	0.25	trace		

[a] Polymerization was carried out at 60 °C for 24 h in THF. [b] Mixture of catalyst and cocatalyst in chlorobenzene was aged for 15 min before use as catalyst. [c] Monomer to catalyst mole ratio. [d] Initial monomer concentration. [e] Methanol-insoluble polymer. [f] Values were obtained by GPC analysis with polystyrene standard calibration.

Table 2. Polymerization of M-II with Various Transition Metal Catalysts[a]

exp. no.	cat. system[b] (mole ratio)	[M]/[C][c]	$[M]_0$[d]	polym yield (%)[e]	$\bar{M}_n \times 10^{-4}$ [f]	$\bar{M}_w/\bar{M}_n$ [f]
1	$MoCl_5$	50	0.25	88	1.8	2.0
2	$MoCl_5$	100	0.25	75	1.4	2.2
3	$MoCl_5$	50	0.5	85	1.7	2.3
4	$MoCl_5$–$(n\text{-Bu})_4Sn$ (1:4)	50	0.25	80	1.5	1.8
5	$MoCl_5$–$EtAlCl_2$ (1:4)	50	0.25	100	1.3	2.1
6	WCl_6	50	0.25	trace		

[a] Polymerization was carried out at 60 °C for 24 h in THF. [b] Mixture of catalyst and cocatalyst in chlorobenzene was aged for 15 min before use as catalyst. [c] Monomer to catalyst mole ratio. [d] Initial monomer concentration. [e] Methanol-insoluble polymer. [f] Values were obtained by GPC analysis with polystyrene standard calibration.

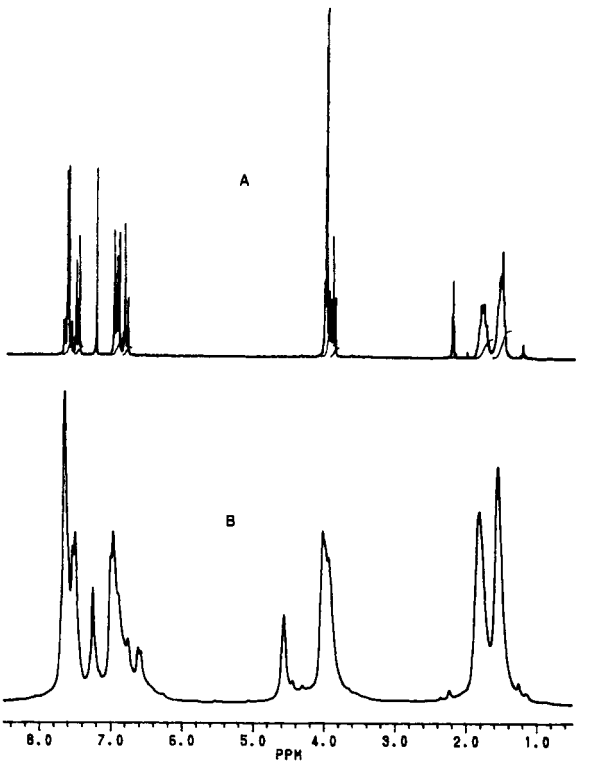

Figure 1. ^1H NMR spectra of M-I (A) and P-I (B) in $CDCl_3$ (sample: exp. no 3 in Table 1).

to the nitrogen atom shifted from 4.0 to 4.4–4.6 ppm on polymerization. The ^{13}C NMR spectra of the monomers gave the acetylenic carbon peaks at 73 and 79 ppm, and the polymers did not show these peaks. Instead, the olefinic carbon peaks of the polymer backbone appeared at about 123 and 137 ppm in the polymers. The peak of the methylene carbon adjacent to the nitrogen atom shifted from 42 to 54 ppm in the polymers. Figure 2 shows the

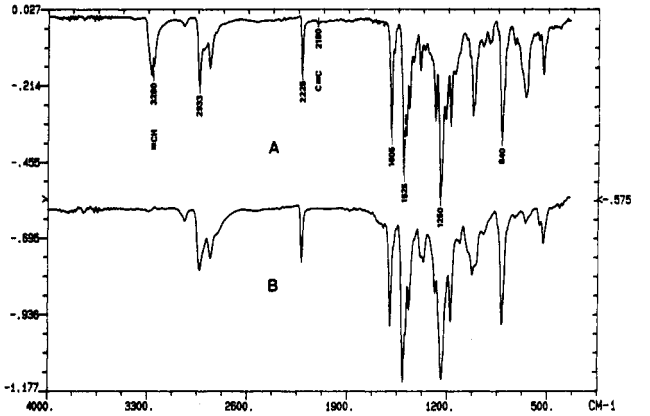

Figure 2. IR spectra of M-I (A) and P-I (B) (KBr pellet) (sample: exp. no 3 in Table 1).

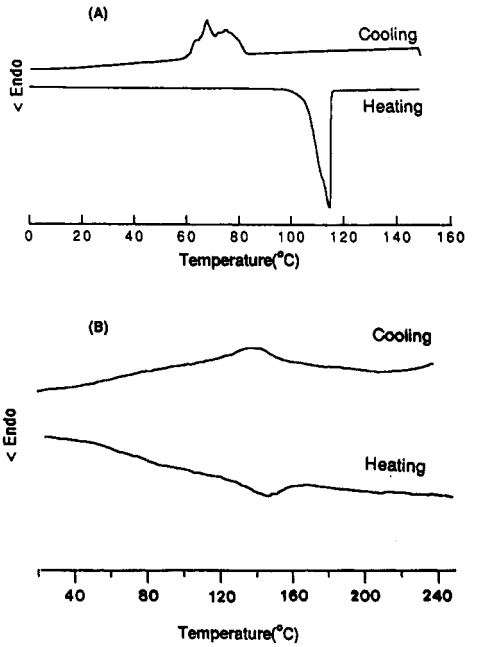

Figure 3. DSC thermograms of M-I (A) and P-I (B) (scanning rate = 10 °C/min) (sample: exp. no. 3 in Table 1).

IR spectra of M-I and P-I. The IR spectrum of P-I shows no absorption at 3280 and 2150 cm^{-1}, which are the characteristic absorption peaks of the acetylenic carbon–hydrogen stretching and carbon–carbon triple-bond stretching of M-I, respectively. The strong band at 2225 cm^{-1} is attributed to the terminal nitrile on the mesogen. The development of the band characteristic of conjugated –C=C– sequences unfortunately cannot be clearly identified, due to the interference in the region of 1605–1650 cm^{-1} of the phenyl ring absorption band dominating the weight of the molecule. UV–visible spectra of all monomers and polymers were obtained in $CHCl_3$. The spectra of the polymers exhibited the characteristic broad absorption bands around 500 nm which were due to the π–π^* transition of the conjugated polyenes.

P-II with its long spacer was highly soluble in various organic solvents such as chloroform, methylene chloride, THF, and 1,4-dioxane and could be cast on glass plates to give a dark-brown film. On the other hand, P-I was partially soluble in various organic solvents because of its short spacer length. However, the obtained polymers were insoluble in *n*-hexane, acetone, diethyl ether, and ethyl acetate. From the above spectral and solubility behavior, it is proposed that the polymer has a cyclized structure (P-I and P-II) as described in Scheme 3.[16,19–21]

Figure 3A shows the DSC thermogram obtained for consecutive heating and cooling cycles on M-I. In the

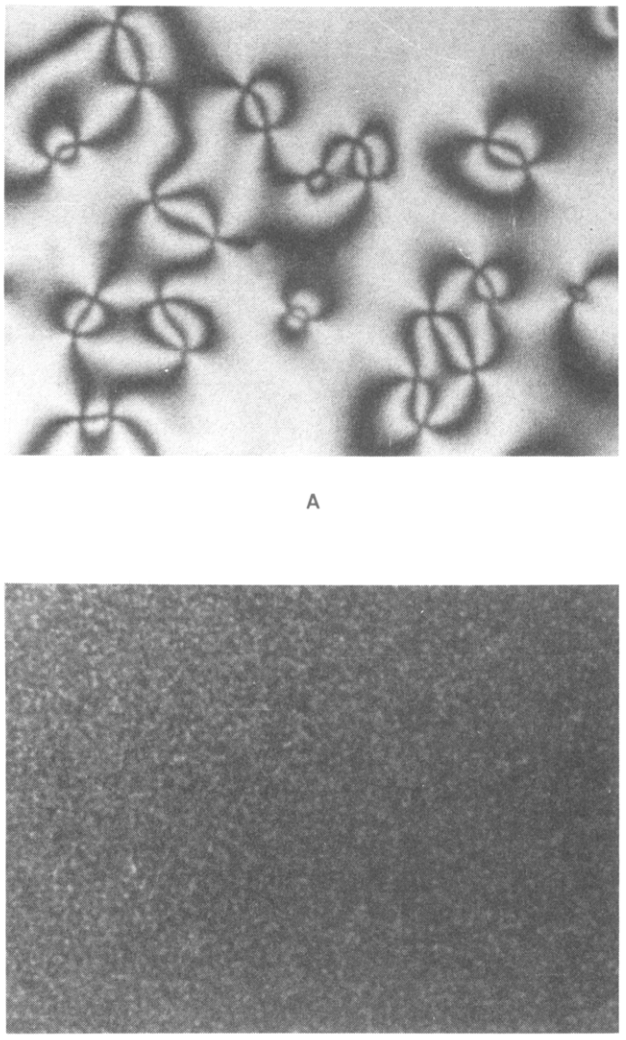

Figure 4. Micrphotographs of M-I (A) taken at 69 °C and P-I (B) taken at 140 °C (sample: exp. no. 3 in Table 1).

second heating, there is a slight shoulder on the isotropization peak between 112 and 115 °C. On cooling, the thermogram contained shoulders at 76 and 68 °C, which may be due to an isotropic to nematic phase transition. Figure 3B presents the second heating and cooling DSC curves of P-I. In the heating and cooling, the glass transition could not be well detected, and only a broad single peak is shown at T_1 = 147 °C (140 °C on the cooling cycle). The transition from the liquid crystalline state to the isotropic state was relatively broad, which is probably due to the high polydispersity and low molecular weight of the polymeric product. Figure 4 shows the photomicrographic properties of the liquid crystalline state of M-I and P-I taken at 69 and 140 °C on cooling cycles, respectively. When M-I was cooled from the isotropic state, a black-and-white schlieren texture formed at 75 °C, and it is characteristic of a typical nematic mesophase. Also, this nematic mixture remained on cooling to room temperature without textural change. In the case of P-I, we observed an undeveloped nematic mesophase on the microphotograph, which was investigated by X-ray analysis.

Figure 5A shows the DSC curves obtained for consecutive heating and cooling cycles of M-II. In the first cooling scan, three exothermic peaks are observed at T_{NI} = 64 °C, T_{SN} = 60 °C, and T_m = 33 °C. The two weak exothermic peaks are due to the transition from the isotropic to the nematic phase (64 °C) and from the nematic to the smectic

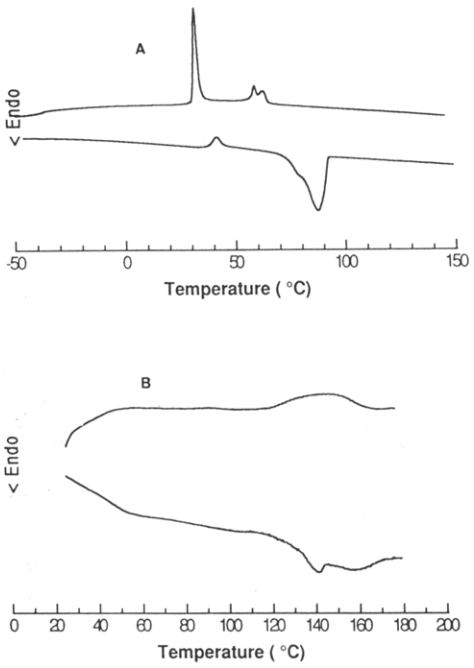

Figure 5. DSC thermograms of M-II (A) and P-II (B) (scanning rate = 10 °C/min) (sample: exp. no. 1 in Table 2).

phase (60 °C), respectively, which were confirmed by microphotographs. The strong exothermic peak at 33 °C is thought to be due to a smectic phase to crystal transition not shown in M-I. It may be due to the influence of decoupling of the mesogenic group with the rigid polyene main chain as a result of the longer methylene spacer in M-II than in M-I. On heating, however, M-II showed a recrystallization exotherm and a larger isotropic endotherm on subsequent heating runs, which implies that it has some semicrystalline character.[22] Figure 5B, which presents the second heating and cooling DSC scans of P-II, indicated well-separated transition regions in the polymer. In the heating point of the DSC curve, P-II exhibits a glass transition at 40 °C, and a nematic transition (T_{SN}) at 141 °C and a broad isotropic transition (T_{NI}) at 159 °C.

Usually, transition temperatures of side-chain LC polymers increase with increasing molecular weight up to limiting values. The molecular weights required for limiting values of T_g and T_i depend on the polymer backbone, spacer chain, and mesogen. Percec, Tomazos, and Pugh[23] reported limiting values of T_g and T_i at $\bar{M}_n > 10^4$ based on GPC with polystyrene standards. Therefore, our results for different molecular weight samples [P-I (0.7×10^4) and P-II (1.8×10^4)] show a similar tendency. Also the solubilities of the polymers increased with increasing spacer chain length, which is more consistent with greater solvation of the mesogens attached to longer spacer chains. Representative polarized optical micrographs of M-II obtained by cooling from the isotropic melt are presented in Figure 6. In M-II, the nematic schlieren texture grows dendritically by slow cooling from the isotropic melt as thready contours (Figure 6A; 63 °C), which merge into droplets on further cooling (Figure 6B; 59 °C). This texture is characteristic of a smectic mesophase. Also, the optical texture of P-II is shown in Figure 6C. A fine-grained texture which was obtained after cooling from the isotropic melt to 110 °C might be a smectic mesophase.[24,25]

The nature of the mesophases was also investigated by X-ray diffraction at room temperature. The diffraction pattern of P-I showed no peak in the small-angle region and a diffuse peak in the wide-angle region (2θ = 20°), characteristic of a nematic mesophase. On the other hand,

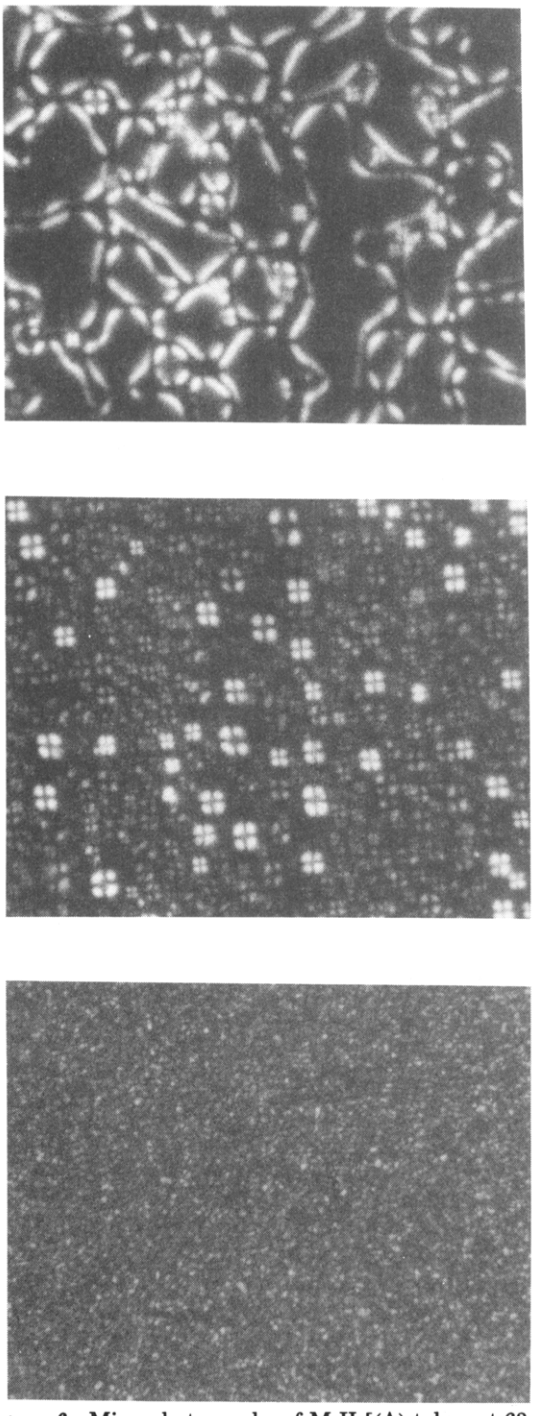

Figure 6. Microphotographs of M-II [(A) taken at 63 °C; (B) taken at 59 °C] and P-II (C) taken at 110 °C] (sample: exp. no. 1 in Table 2).

the X-ray pattern of P-II, attributed to a smectic mesophase, exhibited a narrow peak in the wide-angle region ($2\theta = 20°$) in addition to the sharp peak in the small-angle region ($2\theta = 4.9°$).

Table 3 lists the electrical conductivities of the undoped and I_2-doped polymers. When the film type polymers were exposed to iodine vapor, the electrical conductivity increased from $\sim 10^{-11}$ to $\sim 10^{-3}$ S/cm.

Finally, these results indicate that in the same rigidity of the polymer backbone the length of the flexible spacer plays a significant role in affecting the values of the mesophase transition parameters. The long spacer favors the smectic phase while the short spacer favors the nematic phase. As is true for low molar mass LCs, the tendency toward smectic mesomorphism increases with increasing spacer length.

Table 3. Electrical Conductivities of P-I and P-II[a]

polymer	comp of doped polymer[b]	conductivity[c] (S/cm)
P-I	$(C_{31}H_{30}O_2N_2)_1(I_2)_0$	2.6×10^{-11}
P-I	$(C_{31}H_{30}O_2N_2)_1(I_2)_{0.12}$	7.1×10^{-4}
P-II	$(C_{38}H_{45}O_5N_1)_1(I_2)_0$	4.7×10^{-11}
P-II	$(C_{38}H_{45}O_5N_1)_1(I_2)_{0.17}$	1.8×10^{-3}

[a] These polymers were doped by exposure to iodine vapor under vacuum (1 mmHg) for 2 h. [b] Extent of doping was obtained by weight uptake method. [c] Measured at a frequency of 100 Hz with an applied voltage of 1 V with an Ando AG-4304 LCR meter.

Further research on the change of the UV and electrical conductivity of these polymers in the crystalline temperature range is in progress.

Acknowledgment. We gratefully acknowledge the support of this work by the Korea Science and Engineering Foundation.

References and Notes

(1) McArdle, C. B. *Side Chain Liquid Crystal Polymers*; Blackie: New York, 1989.
(2) Ciferri, A., Krigbaum, W. R., Mayer, R. B., Eds. *Polymer Liquid Crystals*; Academic Press: New York, 1982.
(3) Finkelman, H.; Rehage, G. *Adv. Polym. Sci.* **1984**, *60/61*, 99.
(4) Shibaev, V. P.; Plate, N. A. *Adv. Polym. Sci.* **1984**, *60/61*, 173.
(5) Finkelmann, H.; Ringsdorf, H.; Wendorff, J. H. *Makromol. Chem.* **1978**, *179*, 273.
(6) Finkelmann, H.; Rehage, G. *Makromol. Chem., Rapid Commun.* **1980**, *1*, 31.
(7) Ringsdorf, H.; Scheneller, A. *Makromol. Chem., Rapid Commun.* **1982**, *3*, 557.
(8) Komiya, Z.; Pugh, C.; Schrock, R. R. *Macromolecules* **1992**, *25*, 3609.
(9) Komiya, Z.; Pugh, C.; Schrock, R. R. *Macromolecules* **1992**, *25*, 6586.
(10) Kim, S. H.; Lee, H. J.; Jin, S. H.; Cho, H. N.; Choi, S. K. *Macromolecules* **1993**, *26*, 846.
(11) Pugh, C.; Percec, V. *Polym. Bull.* **1986**, *16*, 513.
(12) Moigne, J. L.; Hilberer, A.; Kajzar, F. *Makromol. Chem.* **1991**, *192*, 515.
(13) Itoh, M.; Lenz, R. W. *J. Polym. Sci., Polym. Chem. Ed.* **1992**, *30*, 803.
(14) Jin, S. H.; Kim, S. H.; Cho, H. N.; Choi, S. K. *Macromolecules* **1991**, *24*, 6050.
(15) Jin, S. H.; Choi, S. J.; Ahn, W. S.; Cho, H. N.; Choi, S. K. *Macromolecules* **1993**, *26*, 1487.
(16) Choi, S. J.; Jin, S. H.; Ahn, W. S.; Cho, H. N.; Choi, S. K. *Macromolecules*, in press.
(17) Hardy, Gy.; Cser, F.; Nyitrai, K.; Samay, G.; Kallo, A. *Magy. Kem. Foly.* **1980**, *86*, 456.
(18) In general, the dipropargylamine gave insoluble polymer in metathesis cyclopolymerization.
(19) Cho, O, K.; Kim, Y. H.; Choi, K. Y.; Choi, S. K. *Macromolecules* **1990**, *23*, 12.
(20) Ryoo, M. S.; Lee, W. C.; Choi, S. K. *Macromolecules* **1990**, *23*, 3029.
(21) Han, S. H.; Kim, U. Y.; Kang, Y. S.; Choi, S. K. *Macromolecules* **1991**, *24*, 973.
(22) Navarro, F.; Serrano, J. L. *J. Polym. Sci., Polym. Chem. Ed.* **1992**, *30*, 1789.
(23) Percec, V.; Tomazos, D.; Pugh, C. *Macromolecules* **1989**, *22*, 3259.
(24) Mallon, J. J.; Kantor, S. W. *Macromolecules* **1990**, *23*, 1249.
(25) Hsieh, C. J.; Hsu, C. S.; Hsiue, G. H.; Percec, V. *J. Polym. Sci., Polym. Chem., Ed.* **1990**, *28*, 425.